B meson semileptonic form factors from unquenched lattice QCD

Emel Gulez,[1] Alan Gray,[1] Matthew Wingate,[2] Christine T. H. Davies,[3] G. Peter Lepage,[4] and Junko Shigemitsu[1]

(HPQCD Collaboration)

[1]*Department of Physics, The Ohio State University, Columbus, Ohio 43210, USA*
[2]*Institute for Nuclear Theory, University of Washington, Seattle, Washington 98195-1550, USA*
[3]*Department of Physics & Astronomy, University of Glasgow, Glasgow, G12 8QQ, United Kingdom*
[4]*Laboratory of Elementary Particle Physics, Cornell University, Ithaca, New York 14853, USA*
(Received 19 January 2006; published 6 April 2006)

The semileptonic process, $B \to \pi l \nu$, is studied via full QCD lattice simulations. We use unquenched gauge configurations generated by the MILC Collaboration. These include the effect of vacuum polarization from three quark flavors: the s quark and two very light flavors (u/d) of variable mass allowing extrapolations to the physical chiral limit. We employ nonrelativistic QCD to simulate the b quark and a highly improved staggered quark action for the light sea and valence quarks. We calculate the form factors $f_+(q^2)$ and $f_0(q^2)$ in the chiral limit for the range $16\ \mathrm{GeV}^2 \leq q^2 < q^2_{\mathrm{max}}$ and obtain $\int_{16\ \mathrm{GeV}^2}^{q^2_{\mathrm{max}}} [d\Gamma/dq^2] dq^2/|V_{ub}|^2 = 1.46(35)\ \mathrm{ps}^{-1}$. Combining this with a preliminary average by the Heavy Flavor Averaging Group (HFAG'05) of recent branching fraction data for exclusive B semileptonic decays from the *BABAR*, Belle and CLEO Collaborations leads to $|V_{ub}| = 4.22(30)(51) \times 10^{-3}$.

DOI: 10.1103/PhysRevD.73.074502 PACS numbers: 12.38.Gc, 13.20.He

I. INTRODUCTION

A major achievement of the B factories in recent years has been the observation of CP violation in the neutral B system [1,2]. The emphasis since then has been on overconstraining the unitarity triangle and checking for consistency with, or deviations from, the three family standard model. The goal is to independently measure not only the three angles but also the lengths of the sides of the triangle and thereby determine $(\bar{\rho}, \bar{\eta})$, the apex of the unitarity triangle, in as many ways as possible. In order to fix the sides of the unitarity triangle, the magnitudes of several Cabibbo-Kobayashi-Maskawa (CKM) matrix elements are required and the accuracy is currently limited mainly by theoretical uncertainties in two of them, $|V_{td}|$ and $|V_{ub}|$. Theory input for these quantities involves hadronic matrix elements of several electroweak operators and these in turn require good control over nonperturbative QCD. This article reports on significant recent progress in lattice QCD determinations of form factors relevant for the CKM matrix element $|V_{ub}|$.

$|V_{ub}|$ can be determined from studies of either inclusive or exclusive B meson semileptonic decays. The first determinations relied on inclusive measurements. However, recent impressive progress in measurements of branching fractions for exclusive decays by CLEO [3], Belle [4,5], and *BABAR* [6–8] have started to make exclusive determinations competitive [9,10]. In either approach, errors are now dominated by theory errors, and which method will eventually win depends on how well the theoretical uncertainties in shape functions (for the inclusive approach) or form factors (in the case of the exclusive approach) can be brought under control. Lattice QCD provides a first principles nonperturbative QCD method for calculating form factors in exclusive semileptonic decays. The first lattice calculations were carried out in the quenched approximation that ignored vacuum polarization effects [11–15]. For some period these pioneering results were the only ones available and experimentalists, e.g. the CLEO Collaboration, used them to extract some of the earliest exclusive $|V_{ub}|$ results [3]. In the summer of 2004 the first preliminary unquenched results for the $B \to \pi l \nu$ form factors were presented by the Fermilab/MILC [16] and HPQCD [17] Collaborations. These calculations employed the MILC Collaboration $N_f = 2 + 1$ unquenched configurations, the most realistic gauge configurations to date with vacuum polarization from 2 flavors of very light quarks and from strange quarks [18]. Furthermore, the good chiral properties of the improved staggered quark action used for the light sea and valence quarks allowed for investigations much closer to the chiral limit than in the earlier calculations. Hence, Refs. [16,17] constitute a major step forward in lattice QCD determinations of semileptonic form factors. These preliminary results have been incorporated by Belle and *BABAR* into their recent B semileptonic analysis [4–8] and used by other theorists in their extractions of $|V_{ub}|$ [19–21].

References [16,17] are part of a growing list of recent lattice calculations that use the MILC unquenched configurations. The creation of these configurations became feasible on present day computers due to the development of highly improved staggered light quark actions [22]. There is one well-known drawback of staggered actions, namely, that each flavor comes in four types, called ''tastes.'' To simulate just one taste of sea quark per flavor, a fourth root of the quark determinant is used and the

validity of this procedure has not yet been rigorously proven. All tests undertaken to date to study the fourth root procedure, however, have led to encouraging results [23]. There are no indications of problems or any deviations from continuum QCD behavior beyond small and expected discretization errors that can be systematically improved upon. A recent review of the fourth root issue is given in [24]. The MILC unquenched configurations and the heavy and light quark actions currently in use have also been tested repeatedly by calculating a large set of well-measured quantities such as light hadron spectroscopy, light meson decay constants, quarkonium, and B meson spectroscopy. Agreement between experiment and lattice calculations is found to be excellent within the few percent errors in the lattice results [25–29]. More impressively, these same gauge configurations have led to some recent predictions from lattice QCD that have been confirmed subsequently by experiment [30–32]. Most relevant for B semileptonic decays is the successful calculation by the Fermilab/MILC Collaboration of D meson semileptonic form factors and the agreement of their q^2 dependence with experiment [32]. All this should boost confidence in results for B meson semileptonic decays that are now emerging from lattice QCD calculations.

In this article we make several further improvements on the preliminary calculations of Ref. [17] and finalize our form factor results. Some of these improvements have been reported in [33]. Among the improvements, we have now included all the dimension 4 current corrections through $\mathcal{O}(\alpha_s/M)$ and $\mathcal{O}(a\alpha_s)$ to the temporal and spatial components of the heavy-light electroweak currents relevant for $B \to \pi l \nu$ semileptonic decays. Our previous results included currents only at lowest order in $1/M$ and through $\mathcal{O}(\alpha_s)$. We now have simulation data from several MILC ensembles, whereas in Ref. [17] results were at a single fixed light sea quark mass and only the valence quark mass was varied. Another development since Ref. [17] is that we now employ the formulas of staggered chiral perturbation theory (SChPT) [34–36] simultaneously to both partially quenched and full QCD results to extrapolate in the light quark mass to the physical pion. Previously we used linear chiral extrapolations to our partially quenched data.

So, the list of improvements in our semileptonic decay studies since the work of Ref. [17] is quite substantial. Nevertheless, we will see that changes in the final results for the form factors $f_+(q^2)$ and $f_0(q^2)$ are almost negligible. The individual contribution from each higher dimension current correction is found to be small, mainly due to small one-loop matching coefficients. There is also some cancellation between the many terms. The difference between linear chiral extrapolations of our previous partially quenched data and results from staggered chiral perturbation theory fits to the new full data set also turns out to be a small effect. With all the improvements now in place, our semileptonic form factor calculations are at the same level as recent B meson decay constant determinations by the HPQCD Collaboration [37,38]. Those latter calculations are crucial for determinations of the CKM matrix elements $|V_{td}|$ and $|V_{ts}|$.

In the next section we provide some details of the simulation parameters and of the lattice actions employed. We also summarize formulas for the relevant form factors. In Sec. III we discuss matching of the lattice heavy-light currents used in our simulations to their continuum QCD counterparts. One-loop matching coefficients for the temporal components V_0 and A_0 were published in Ref. [39] and have been used already in our decay constant determinations [37,38]. Matching of the spatial components V_k was completed as part of the current project. Section IV describes how we extract the form factors $f_\parallel$ and $f_\perp$ from numerical simulations. The more commonly used form factors f_+ and f_0 can be expressed as simple linear combinations of $f_\parallel$ and $f_\perp$. Section V focuses on chiral extrapolations of $f_\parallel$ and $f_\perp$. In Sec. VI we summarize our final results for $f_+(q^2)$ and $f_0(q^2)$ in the physical chiral limit. We also present tables of partially integrated differential decay rates (divided by $|V_{ub}|^2$) in several q^2 bins. In Sec. VII we combine the results of Sec. VI with experimental data on $B \to \pi l \nu$ branching fractions to estimate $|V_{ub}|$. We then conclude with a summary section.

II. SIMULATION DETAILS AND FORM FACTOR FORMULAS

Most of our simulations were performed on the MILC Collaboration ''coarse'' ensembles with lattice spacing around 0.12 fm and with light sea quark masses in units of the strange quark mass, m_f/m_s, ranging between 0.125 and 0.5. We have also carried out some checks using MILC lattices with finer lattice spacings. We refer to the original papers by the MILC Collaboration for details of how their lattices were generated [18]. Some specifications for the

TABLE I. Simulation details. m_f (m_q) denotes sea (valence) quark masses and m_s is the strange quark mass. A † means the lattice spacing was determined through r_1. For all other ensembles the Υ 2S-1S splitting was used. $u_0 = [\text{plaq}]^{1/4}$ is the link variable that enters into the MILC Collaboration's convention for normalization of quark masses.

$N_s^3 \times N_t$	a^{-1} (GeV)	N_{conf}	$u_0 a m_f$	$u_0 a m_q$	m_q/m_s
Coarse					
$24^3 \times 64$	1.623(32)†	399	0.005	0.005	0.125
$20^3 \times 64$	1.622(32)†	397	0.007	0.007	0.175
$20^3 \times 64$	1.596(30)	568	0.010	0.005	0.125
				0.010	0.250
				0.020	0.500
$20^3 \times 64$	1.605(29)	486	0.020	0.020	0.500
Fine					
$28^3 \times 96$	2.258(32)	465	0.0062	0.0062	0.200
$28^3 \times 96$	2.312(31)	496	0.0124	0.0124	0.400

ensembles are given in Table I. The highly improved staggered action, the AsqTad action, is used for both the sea and valence light quarks. The leading discretization errors in this formalism are $\mathcal{O}(a^2\alpha_s)$. To simulate the b quark inside the B meson we use the same highly improved nonrelativistic QCD (NRQCD) action employed in recent studies of the Υ system on the same MILC ensembles [28,40]. In terms of the two-component Pauli spinor Φ one has

$$\mathcal{L}_{\mathrm{NRQCD}} = \sum_x \Big\{ \Phi_t^\dagger \Phi_t - \Phi_t^\dagger \Big(1 - \frac{a\delta H}{2}\Big)_t \Big(1 - \frac{aH_0}{2n}\Big)_t^n \times \frac{1}{u_0} U_t^\dagger (t-1) \Big(1 - \frac{aH_0}{2n}\Big)_{t-1}^n \times \Big(1 - \frac{a\delta H}{2}\Big)_{t-1} \Phi_{t-1} \Big\}, \quad (1)$$

where n is a stability parameter introduced to control high momentum modes of the b propagator [28]. H_0 is the nonrelativistic kinetic energy operator,

$$H_0 = -\frac{\Delta^{(2)}}{2M_0}, \quad (2)$$

and δH includes relativistic and finite-lattice-spacing corrections,

$$\delta H = -c_1 \frac{(\Delta^{(2)})^2}{8M_0^3} + c_2 \frac{ig}{8M_0^2}(\nabla \cdot \tilde{\mathbf{E}} - \tilde{\mathbf{E}} \cdot \nabla) - c_3 \frac{g}{8M_0^2} \boldsymbol{\sigma} \cdot (\tilde{\nabla} \times \tilde{\mathbf{E}} - \tilde{\mathbf{E}} \times \tilde{\nabla}) - c_4 \frac{g}{2M_0} \boldsymbol{\sigma} \cdot \tilde{\mathbf{B}} + c_5 \frac{a^2 \Delta^{(4)}}{24 M_0} - c_6 \frac{a(\Delta^{(2)})^2}{16 n M_0^2}. \quad (3)$$

M_0 is the bare b quark mass, $\Delta^{(2)}$ the lattice Laplacian, ∇ the symmetric lattice derivative and $\Delta^{(4)}$ the lattice discretization of the continuum $\sum_i D_i^4$. Expressions for the improved $\tilde{\mathbf{E}}$ and $\tilde{\mathbf{B}}$ fields are given in [28]. All derivatives are tadpole improved. As in [28] we set the c_i's to their tree level value, $c_i = 1$. These coefficients will be modified by radiative corrections at higher order. For heavy-light systems the most important radiative corrections will be to c_4. All other c_i's are multiplied by additional factors of $1/M$ or a. Based on the discussions in [28] we estimate the effect from radiative corrections to c_4 on B semileptonic form factor calculations to be less than 1%.

Just as in continuum QCD, our lattice actions include a small number of parameters that can only be fixed via experimental input. These are the bare quark mass parameters and the scale (or coupling). For the present case of heavy-light simulations the action parameters have already been fixed for us via simulations of quarkonium and light quark systems using the same MILC configurations. We use lattice spacings determined by the Υ 2S-1S splitting [28]. For two of the MILC ensembles (denoted by a † in Table I), Υ simulations have not yet been carried out. On the other hand, the MILC Collaboration has measured the heavy quark potential parameter r_1/a (in lattice units) for these ensembles [26]. In Ref. [28], using MILC ensembles on which both r_1/a and the Υ 2S-1S splittings were calculated, we could use the experimental 2S-1S splitting to determine $r_1 = 0.321(5)$ fm. This physical value for r_1 was combined with the MILC Collaboration's r_1/a to fix the scale for the above two ensembles. The b quark mass is also fixed by our Υ studies. Studies of pions and kaons have fixed the u and d masses (which we take to be equal to each other) and the s quark mass, respectively [26,27]. Hence by the time one gets to the B system there are no adjustable parameters left in our QCD action.

To study the process $B \to \pi l \nu$, one needs to evaluate the matrix element of the charged electroweak current between the B and the π states, $\langle \pi | (V-A)^\mu | B \rangle$. Only the vector current V^μ contributes to the pseudoscalar-to-pseudoscalar amplitude and the matrix element can be written in terms of two form factors $f_+(q^2)$ and $f_0(q^2)$. These depend only on the square of the momentum transferred between the B and the π, $q^\mu = p_B^\mu - p_\pi^\mu$.

$$\langle \pi(p_\pi) | V^\mu | B(p_B) \rangle = f_+(q^2) \Big[p_B^\mu + p_\pi^\mu - \frac{M_B^2 - m_\pi^2}{q^2} q^\mu \Big] + f_0(q^2) \frac{M_B^2 - m_\pi^2}{q^2} q^\mu. \quad (4)$$

If one neglects the mass of the charged lepton in the final state, only the form factor $f_+(q^2)$ contributes to the decay rate $\Gamma(B \to \pi l \nu)$. Nevertheless, it is useful to keep track of the form factor $f_0(q^2)$ as well since, as we shall see, it helps in our interpolations and extrapolations of simulation data. In our data analysis another pair of form factors, $f_\parallel$ and $f_\perp$, turns out to be more convenient.

$$\langle \pi(p_\pi) | V^\mu | B(p_B) \rangle = \sqrt{2M_B} [v^\mu f_\parallel + p_\perp^\mu f_\perp], \quad (5)$$

with

$$v^\mu = \frac{p_B^\mu}{M_B}, \qquad p_\perp^\mu = p_\pi^\mu - (p_\pi \cdot v) v^\mu. \quad (6)$$

In the B rest frame (in this article we only consider B mesons decaying at rest) the temporal and spatial parts of (5) become

$$\langle \pi | V^0 | B \rangle = \sqrt{2M_B} f_\parallel, \qquad \langle \pi | V^k | B \rangle = \sqrt{2M_B} p_\pi^k f_\perp. \quad (7)$$

Hence, one sees that one can separately determine $f_\parallel$ or $f_\perp$ simply by looking at either the temporal or spatial component of V^μ. These two form factors have the additional advantage that they have simpler heavy quark effective theory scaling properties and chiral perturbation theory (ChPT) is carried out in terms of them rather than for f_+ and f_0. After carrying out the chiral extrapolations for $f_\parallel$ and $f_\perp$, we convert back to obtain f_+ and f_0 for the physical theory using

$$f_+ = \frac{1}{\sqrt{2M_B}} f_\parallel + \frac{1}{\sqrt{2M_B}} (M_B - E_\pi) f_\perp, \quad (8)$$

$$f_0 = \frac{\sqrt{2M_B}}{(M_B^2 - m_\pi^2)} [(M_B - E_\pi) f_\parallel + (E_\pi^2 - m_\pi^2) f_\perp], \quad (9)$$

where E_π is the pion energy in the B rest frame. From these formulas one sees that f_+ will be dominated by $f_\perp$, i.e. by the matrix element of V_k, and f_0 by $f_\parallel$ or the matrix element of V_0.

Our goal is to evaluate the hadronic matrix elements $\langle\pi|V^0|B\rangle$ and $\langle\pi|V^k|B\rangle$ via lattice simulations. There are several steps in the calculation. First, one must relate the continuum electroweak currents, V^0 and V^k, to lattice operators written in terms of the heavy and light quark fields in our lattice actions. In the second step the matrix elements of these lattice current operators must be evaluated numerically and the relevant amplitude, i.e. the matrix element between the ground state B meson and the ground state pion with appropriate momenta, must be extracted. This will give us, via Eqs. (7), the form factors $f_\parallel$ and $f_\perp$ as functions of the light quark mass and the pion momentum. Finally, in step 3 these numerical results must be extrapolated to the physical pion. In the next three sections we describe each of these three steps in turn.

III. MATCHING OF HEAVY-LIGHT CURRENTS

Matching of heavy-light currents between continuum QCD and a lattice effective theory with two-component nonrelativistic heavy quark fields Φ and four-component light quarks $q(x)$ is discussed in Ref. [41]. Since staggered light quarks can be written in terms of four-component "naive" AsqTad quark fields the formalism developed there carries over unchanged to the present calculation. Introducing also a four-component notation for the heavy field, $Q(x) \equiv (\Phi, 0)$, one finds that through $\mathcal{O}(\alpha_s\Lambda_{\rm QCD}/M, \alpha_s/(aM), \alpha_s a\Lambda_{\rm QCD})$ the following current operators in the effective theory are required.

Temporal:

$$\begin{aligned} J_0^{(0)}(x) &= \bar{q}(x)\Gamma_0 Q(x), \\ J_0^{(1)}(x) &= \frac{-1}{2M_0}\bar{q}(x)\Gamma_0\boldsymbol{\gamma}\cdot\boldsymbol{\nabla}Q(x), \\ J_0^{(2)}(x) &= \frac{-1}{2M_0}\bar{q}(x)\boldsymbol{\gamma}\cdot\overleftarrow{\boldsymbol{\nabla}}\gamma_0\Gamma_0 Q(x). \end{aligned} \tag{10}$$

Spatial:

$$\begin{aligned} J_k^{(0)}(x) &= \bar{q}(x)\Gamma_k Q(x), \\ J_k^{(1)}(x) &= \frac{-1}{2M_0}\bar{q}(x)\Gamma_k\boldsymbol{\gamma}\cdot\boldsymbol{\nabla}Q(x), \\ J_k^{(2)}(x) &= \frac{-1}{2M_0}\bar{q}(x)\boldsymbol{\gamma}\cdot\overleftarrow{\boldsymbol{\nabla}}\gamma_0\Gamma_k Q(x), \\ J_k^{(3)}(x) &= \frac{-1}{2M_0}\bar{q}(x)\nabla_k Q(x), \\ J_k^{(4)}(x) &= \frac{1}{2M_0}\bar{q}(x)\overleftarrow{\nabla}_k Q(x), \end{aligned} \tag{11}$$

where Γ_μ can be either γ_μ or $\gamma_5\gamma_\mu$, and M_0 is the bare heavy quark mass in the NRQCD action. One sees that there are two dimension 4 current corrections to the temporal components and four such corrections to the spatial components. To the order that we are working, one has

$$\begin{aligned} \langle V_0\rangle = (1 + \alpha_s\tilde{\rho}_0^{(0)})\langle J_0^{(0)}\rangle + (1 + \alpha_s\rho_0^{(1)})\langle J_0^{(1),\rm sub}\rangle \\ + \alpha_s\rho_0^{(2)}\langle J_0^{(2)}\rangle \end{aligned} \tag{12}$$

and

$$\begin{aligned} \langle V_k\rangle = (1 + \alpha_s\tilde{\rho}_k^{(0)})\langle J_k^{(0)}\rangle + (1 + \alpha_s\rho_k^{(1)})\langle J_k^{(1),\rm sub}\rangle \\ + \alpha_s\rho_k^{(2)}\langle J_k^{(2)}\rangle + \alpha_s\rho_k^{(3)}\langle J_k^{(3)}\rangle + \alpha_s\rho_k^{(4)}\langle J_k^{(4)}\rangle. \end{aligned} \tag{13}$$

We introduce the combination $J_\mu^{(1),\rm sub} = J_\mu^{(1)} - \alpha_s\zeta_{10,\mu}J_\mu^{(0)}$. This subtracts out power law contributions to the matrix elements of the higher dimension operator $J_\mu^{(1)}$ through $\mathcal{O}(\alpha_s/(aM))$ [42]. $J_\mu^{(1)}$ enters the matching already at tree level and after the subtraction one is left with the physical $\mathcal{O}(\Lambda_{\rm QCD}/M)$ contribution that is a relativistic correction to the leading order term. Power law subtractions of the other dimension 4 current corrections come in as $\mathcal{O}(\alpha_s^2/(aM))$ effects and are only partially included here. The one-loop coefficients $\rho_\mu^{(j)}$ and $\zeta_{10,\mu}$ for $\mu = 0$ are given in Ref. [39].

TABLE II. Matching coefficients for the spatial currents V_k. Where errors are not indicated explicitly, they are of order one or less in the last digit. aM_0 is the bare heavy quark mass in lattice units and n a parameter in the NRQCD action. The three selected values for aM_0 correspond to the b quark on the MILC extra-coarse, coarse and fine lattices, respectively [28].

aM_0	n	$\tilde{\rho}_k^{(0)}$	$\rho_k^{(1)}$	$\rho_k^{(2)}$	$\rho_k^{(3)}$	$\rho_k^{(4)}$	$\zeta_{10,k}$
4.00	2	0.256	0.484(3)	0.340(6)	0.244(3)	−0.137(3)	0.041
2.80	2	0.270	0.349(3)	0.169(6)	0.218(4)	−0.029(4)	0.055
1.95	2	0.332	0.232(3)	0.121(8)	0.161(4)	0.063(3)	0.073

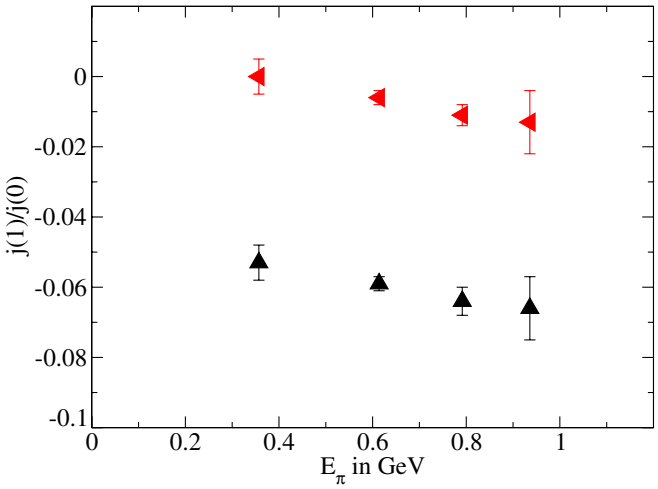

FIG. 1 (color online). The ratio $\langle J_0^{(1)}\rangle/\langle J_0^{(0)}\rangle$ for one ensemble ($u_0 am_f = u_0 am_q = 0.01$) versus the pion energy E_π. The lower points are before power law subtraction and the upper points are after power law subtraction (i.e. $\langle J_0^{(1),\rm sub}\rangle/\langle J_0^{(0)}\rangle$).

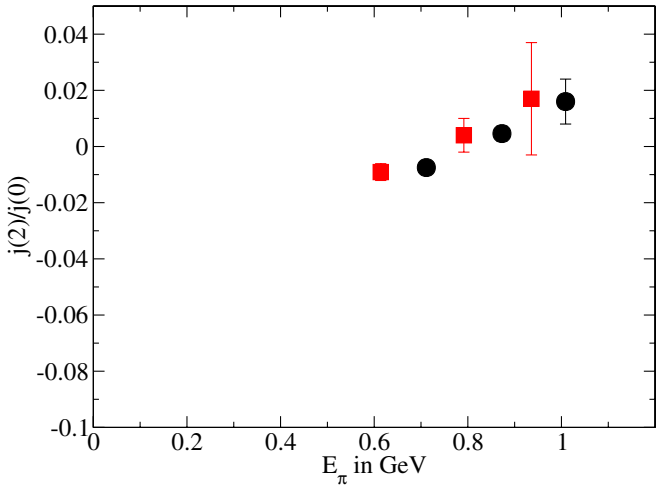

FIG. 2 (color online). The ratio $\langle J_k^{(2)}\rangle/\langle J_k^{(0)}\rangle$ for two ensembles versus the pion energy E_π. Squares are for $u_0 am_f = 0.01$ and circles for $u_0 am_f = 0.02$.

The results for $\mu = k$ have not been published before and are summarized in Table II. In Ref. [17] only the contributions from the first terms in Eqs. (12) and (13) were taken into account, i.e. $J_0^{(0)}$ and $J_k^{(0)}$ matched through $\mathcal{O}(\alpha_s)$.

As mentioned in the Introduction, the effects of all the dimension 4 current corrections turn out to be very small. In Fig. 1 we show results for $\langle J_0^{(1)}\rangle/\langle J_0^{(0)}\rangle$ for one of our ensembles with and without the power law subtraction. One sees that, although the unsubtracted $\langle J_0^{(1)}\rangle/\langle J_0^{(0)}\rangle$ is at the $\sim$6% level, the physical $\langle J_0^{(1),\mathrm{sub}}\rangle/\langle J_0^{(0)}\rangle$ is $\leq 1\%$. In Figs. 2–4 we give further examples of $\langle J_k^{(j)}\rangle/\langle J_k^{(0)}\rangle$ for $j > 1$. These get multiplied by factors of $(\rho_k^{(j)}\alpha_s)$ in Eq. (13). Using $\alpha_s \approx \alpha_V(2/a) = 0.32$ [43] and Table III, one finds $\rho\alpha_s$ factors between 0.01 and 0.11, which leads to contributions from higher order currents that are at most 1%. For instance, the largest current correction is $J_k^{(4)}$ (Fig. 4), but $\rho_k^{(4)}\alpha_s = -0.029\alpha_s = -0.0009$, and the contribution from this current is negligible. In comparing Figs. 1–4 one sees that the size of the matrix elements grows with the pion energy E_π for $J_k^{(2)}$ and $J_k^{(4)}$ and seems much less sensitive to E_π for the other two currents. This reflects the fact that $J_k^{(2)}$ and $J_k^{(4)}$ have derivatives acting on the light quark field that is part of the final state pion and therefore knows about its momentum.

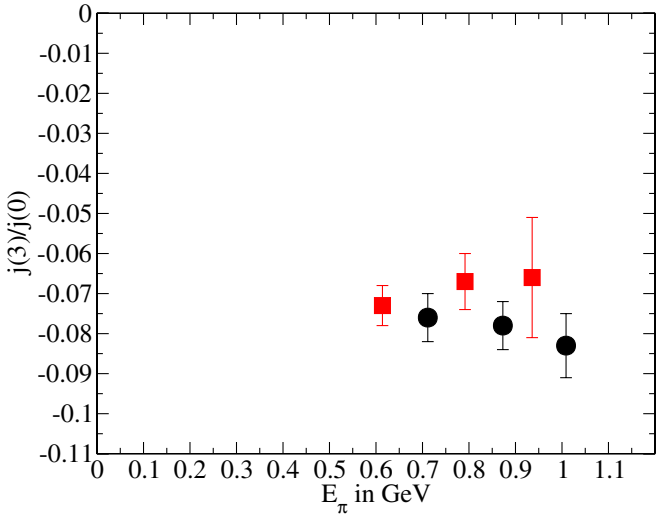

FIG. 3 (color online). Same as Fig. 2 for $\langle J_k^{(3)}\rangle/\langle J_k^{(0)}\rangle$.

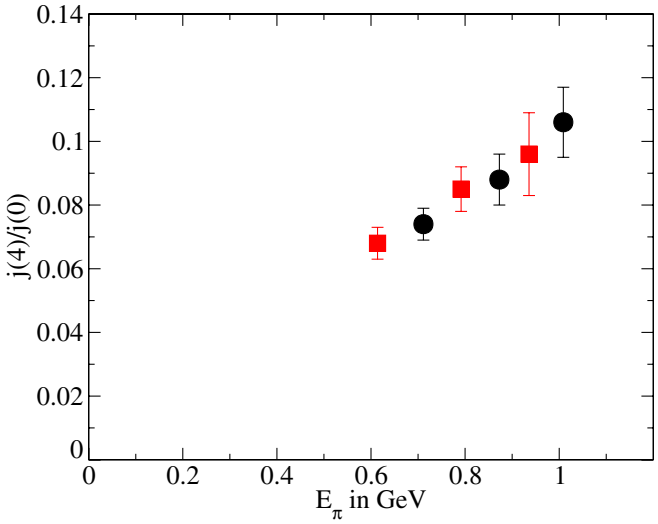

FIG. 4 (color online). Same as Fig. 2 for $\langle J_k^{(4)}\rangle/\langle J_k^{(0)}\rangle$.

IV. SIMULATION RESULTS FOR FORM FACTORS $f_\parallel$ AND $f_\perp$

The starting point for calculations of the hadronic matrix elements $\langle\pi|J_\mu^{(j)}|B\rangle$ is the 3-point correlator

$$C^{(3)}(\vec{p}_\pi, \vec{p}_B, t, T_B) = \sum_{\vec{z}}\sum_{\vec{y}}\langle\Phi_\pi(0)J_\mu^{(j)}(\vec{z}, t)\Phi_B^\dagger(\vec{y}, -T_B)\rangle \times e^{i\vec{p}_B\cdot\vec{y}}e^{i(\vec{p}_\pi-\vec{p}_B)\cdot\vec{z}}, \quad (14)$$

where Φ_B and Φ_π are interpolating operators for the B meson and the pion, respectively. All results here have the B meson three momentum, $\vec{p}_B$, set equal to zero. For simplicity, the pion operator Φ_π was always placed at the origin. The B meson was then created at time slice $-T_B$ and the electroweak current, $J_\mu^{(k)}$, that converts the b quark into a u quark was inserted at times $0 \geq t \geq -T_B$. We have also simulated the time-reversed process, which then has the electroweak current inserted between $+T_B \geq t \geq 0$ and Φ_B acting on time slice $+T_B$. By looking at both forward and time-reversed processes and verifying that they lead to consistent results (within statistical errors), we were able to increase statistics and at the same time provide some check on our codes. For most of our simulations we used $T_B/a = 16$ on the coarse MILC lattices

and $T_B/a = 24$ on the fine lattices. On one of the coarse lattices we also ran with $T_B/a = 20$ and verified that results for form factors were independent of T_B. Making T_B too large is not helpful since statistical errors grow with T_B. On the other hand, making T_B too small limits the number of data points available and gives us less flexibility in our fits.

In constructing the interpolating operators Φ_B and Φ_π we have found it convenient, just as in the currents of Eqs. (10) and (11), to work with four-component naive fields $q(x)$ rather than one-component staggered fields $\chi(x)$. Hence in Eq. (14) we use

$$\Phi_B^\dagger = \bar{Q}\gamma_5 q, \qquad \Phi_\pi = \bar{q}\gamma_5 q. \tag{15}$$

The relation between naive and staggered fermion propagators is given by [44]

$$G_q(x, y) = \Omega(x)\Omega^\dagger(y)G_\chi(x, y) \tag{16}$$

with

$$\Omega(x) = \prod_{\mu=0}^{3}(\gamma_\mu)^{x_\mu}. \tag{17}$$

In our simulations we first calculate staggered propagators G_χ, since they are cheaper, and then convert to naive propagators G_q using Eq. (16) before evaluating 3-point correlators. The naive AsqTad theory has 16 tastes of quark per flavor and hence one could form 16 different heavy-light pseudoscalar bound states. However, as discussed in Ref. [44] these exactly degenerate 16 B mesons do not mix and the 2-point correlator $\langle\Phi_B(x)\Phi_B^\dagger(y)\rangle$, for instance, receives contributions from only one of these possible B mesons. Similarly one can argue that in Eq. (14) only one type of B meson is involved and that it connects to only one of the 16 true Goldstone pions of the naive light quark theory (out of a total number of 256 pions). In other words, both Eq. (14) and the Φ_B 2-point correlator have the same normalization as in a theory with undoubled light and heavy quarks, such as continuum QCD. The one correlator where adjustment of normalization is required is the $\Phi_\pi - \Phi_\pi$ correlator. Using naive fields as in Eq. (15) brings in an extra factor of 16 due to the trace over a 16×16 taste matrix and this factor of 16 must be divided out. If one works with conventional staggered light quarks one would have an extra factor of 4 rather than 16 relative to a pion correlator in a theory with undoubled fermions.

To extract the matrix elements $\langle\pi|J_\mu^{(j)}(t)|B\rangle$, the 3-point correlators must be fitted to

$$C^{(3)}(\vec{p}_\pi, \vec{p}_B, t, T_B) \to \sum_{k=0}^{N_\pi-1}\sum_{l=0}^{N_B-1}(-1)^{k*t} \times (-1)^{l*(T_B-t)}A_{\mu,lk}^{(j)}e^{-E_\pi^{(k)}t}e^{-E_B^{(l)}(T_B-t)}. \tag{18}$$

With this ansatz every second exponential (k or l odd) corresponds to an oscillatory (in time) contribution to the correlator, a characteristic feature of staggered fermions. We use Bayesian fitting methods [45] and in most of our fits we kept $N_\pi = 1$ and let N_B vary between 3 and 9. In order to avoid contamination from excited pions we dropped 5 to 8 points close to the pion source and made certain that within errors fit results did not depend on the number of points omitted. We have also tried some fits with $N_\pi = 2$ or 3. For some light quark masses and pion momenta one obtained results consistent with the $N_\pi = 1$ fits; in other cases, however, it was not possible to get very stable (with respect to N_B) fits. Hence, for our final results we rely on the $N_\pi = 1$ fits. Since oscillatory contributions are much more significant in the B channel than for pions, it was more important to allow N_B to increase at fixed N_π rather than the other way around. For priors in our Bayesian fits we use central values corresponding to energy splittings of about 400 MeV allowing, however, for large $\sim$100% widths. As priors for the amplitudes we allow for ranges typically between about $-10 \times A_{00}$ and $+10 \times A_{00}$, where A_{00} is the ground-state amplitude. Fit results for ground-state energies and amplitudes were very insensitive to choices for priors. In Figs. 5 and 6 we show examples of fit results for $\langle J_\mu^{(0)}(t)\rangle$ for pion momentum $\frac{2\pi}{N_s a}(0, 1, 1)$ on one of the coarse ensembles. For comparison we show in Fig. 7 results for a fit to the B correlator that was done simultaneously with the fit to the 3-point correlator.

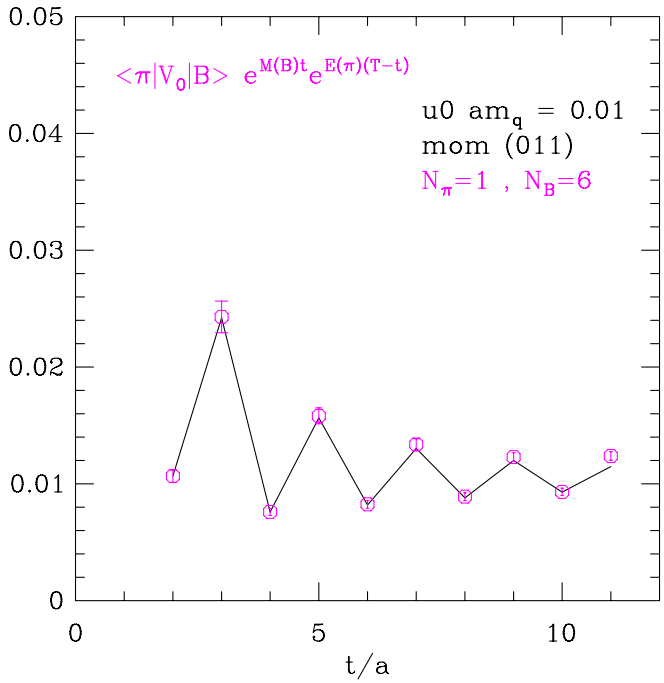

FIG. 5 (color online). Fit result for $\langle J_0^{(0)}(t)\rangle \times e^{M_B t} \times e^{E_\pi(T-t)}$ versus t for pion momentum $(0, 1, 1)\frac{2\pi}{N_s a}$. The horizontal time axis has been rearranged so that the B meson source is at $t/a = 1$ and the pion source at $t/a = T = 16$.

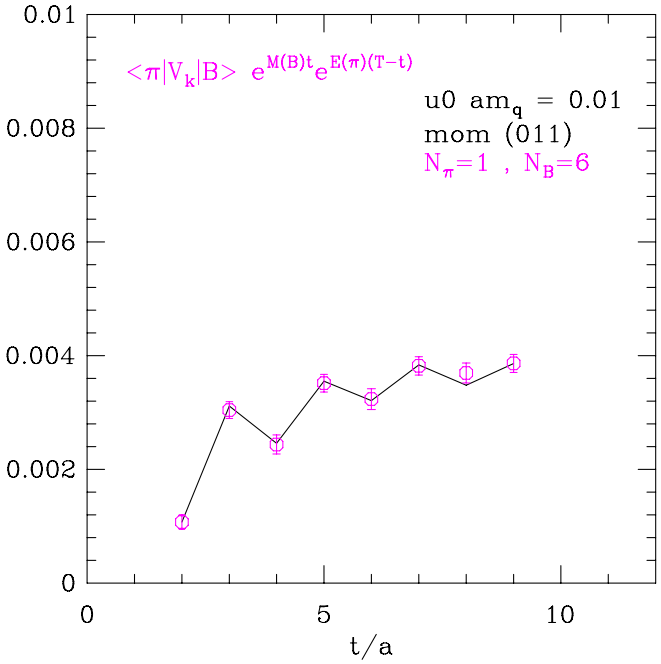

FIG. 6 (color online). Same as Fig. 5 but for $\langle J_k^{(0)}(t)\rangle$.

The main goal in all our fits is to extract the ground-state amplitudes $A^{(j)}_{\mu,00}$ which lead directly to the form factors $f_\parallel$ and $f_\perp$ via Eq. (7).

$$f_\parallel = \frac{A_{00}(V_0)}{\sqrt{\zeta_\pi \zeta_B}}\sqrt{2E_\pi}, \qquad f_\perp = \frac{A_{00}(V_k)}{\sqrt{\zeta_\pi \zeta_B p_\pi^k}}\sqrt{2E_\pi}. \quad (19)$$

Here $A_{00}(V_\mu)$ includes contributions from all currents with

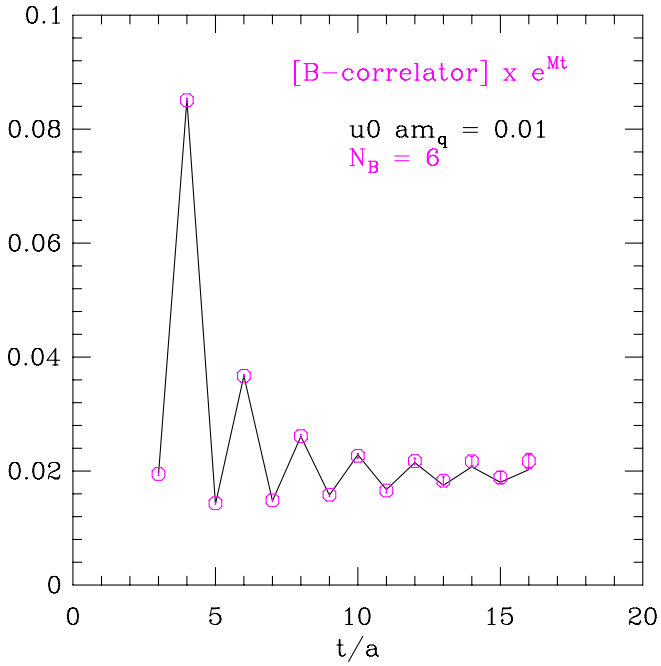

FIG. 7 (color online). Fit results for the *B* meson correlator.

TABLE III. Results for the form factor $f_\parallel$ in GeV$^{1/2}$ from coarse MILC lattices. Errors are statistical errors coming from Bayesian bootstrap fits.

u_0am_f	u_0am_q	p_π = (000)	(001)	(011)	(111)
0.005	0.005	1.486(34)	1.326(36)	1.221(38)	1.127(78)
0.007	0.007	1.538(32)	1.328(33)	1.185(49)	1.013(115)
0.010	0.005	1.582(37)	1.322(37)	1.201(60)	1.053(121)
0.010	0.010	1.584(44)	1.322(39)	1.212(52)	1.064(138)
0.010	0.020	1.581(30)	1.372(29)	1.253(37)	1.117(72)
0.020	0.020	1.508(48)	1.378(43)	1.264(47)	1.121(83)

TABLE IV. Same as Table III for the form factor $f_\perp$ in GeV$^{-1/2}$.

u_0am_f	u_0am_q	p_π = (001)	(011)	(111)
0.005	0.005	1.543(205)	0.703(44)	0.515(39)
0.007	0.007	1.082(31)	0.606(31)	0.433(48)
0.010	0.005	1.128(37)	0.662(36)	0.413(38)
0.010	0.010	1.235(90)	0.657(37)	0.449(43)
0.010	0.020	1.029(21)	0.611(19)	0.423(23)
0.020	0.020	1.097(140)	0.597(24)	0.397(20)

appropriate matching factors as dictated by Eqs. (12) and (13). ζ_π and ζ_B are the ground-state amplitudes from the pion and *B* meson correlators, respectively. ζ_π is correctly normalized as in continuum QCD. Results for the form factors $f_\parallel$ and $f_\perp$ for the different ensembles and pion momenta are summarized in Tables III and IV.

V. CHIRAL EXTRAPOLATIONS

The form factors listed in Tables III and IV are for an unphysical world with *u* and *d* quark masses larger than in reality. They need to be extrapolated to the physical chiral limit. In Ref. [17] linear extrapolations were performed on the three points with $u_0am_f = 0.01$, the only simulation data available at that time. Here we carry out this important step in several different ways: (1) linear extrapolation with only the full QCD ($m_f = m_q$) data, (2) SChPT with full QCD data, (3) continuum ChPT with full QCD data, and (4) SChPT simultaneously to both full QCD and partially quenched data. We use the last, most involved chiral extrapolation for our final answer, but make certain that the other methods give agreement within quoted errors.

The formulas of chiral perturbation theory for heavy-light form factors have the general form

$$f_{\parallel/\perp} = c_0[1 + \delta f_{\parallel/\perp} + c_1 m_q + c_2(2m_f + m_s) + \ldots]. \quad (20)$$

$\delta f_\parallel$ and $\delta f_\perp$ are the chiral log terms and they have been determined at lowest order in $1/M$ for continuum, quenched and partially quenched QCD [46,47] and also specifically for staggered light quarks [34–36]. We use the

formulas of Aubin and Bernard [36] that include "taste symmetry breaking" lattice artifact terms that come in at $\mathcal{O}(a^2)$. $\delta f_\parallel$ and $\delta f_\perp$ are functions of E_π (more generally of $v \cdot p_\pi$, with v^μ equal to the B four velocity and p_π^μ the pion momentum) and also depend on the $B^* B\pi$ coupling $g_{B\pi}$. A possible source of concern in using ChPT may be the presence of pions with $E_\pi > 2m_\pi$ in our system. Higher order terms in continuum heavy-light ChPT are discussed, for instance, in Ref. [48]. There it is argued that, for some processes, effects of higher order terms can be taken into account by allowing for a correction to $g_{B\pi}$ linear in E_π. In our fits to SChPT and to continuum ChPT formulas we will let $g_{B\pi}$ vary as one goes from one E_π value to another, together with c_0, c_1 and c_2.

The discussion in the previous paragraph shows that chiral extrapolations are most conveniently carried out at fixed values of E_π. In order to do so, one needs to interpolate the data of Tables III and IV to fixed common values of E_π for each light quark mass. We have explored several different ways to perform the interpolations. We take advantage of various ansaetze that have been developed in the literature to model the q^2 dependence of form factors $f_+(q^2)$ and $f_0(q^2)$. The Appendix summarizes commonly used ansaetze [19–21,49–52]. The formulas given there refer to form factors in the real world, i.e. when using physical values for pion, B and B^* masses. We use them here also as guides for sensible interpolations even at unphysical meson masses. We caution, however, that quantities such as $q^2_{\rm max} = (M_B - m_\pi)^2$, $M^2_{B^*} - q^2_{\rm max}$ or the $B\pi$ threshold $(M_B + m_\pi)^2$ are sensitive to the pion mass. A particular ansatz may not work as well with unphysical masses compared to in the chiral limit, or vice versa. For instance, we find that away from the chiral limit, i.e. when we are interpolating the data of Tables III and IV, the most popular 3 parameter Becirevic-Kaidalov (BK) ansatz [49] often fails to accommodate our data. After the chiral extrapolation the BK ansatz works well, however. On the other hand, we were often (though not always) able to fit data away from the chiral limit using just a simple single pole ansatz for both f_0 and f_+, but, as expected, a single pole ansatz does not work for $f_+(q^2)$ in the physical limit. The ansatz that works best both away from and at the chiral limit is one due to Ball and Zwicky (BZ) [50], which actually is the same as the 4 parameter BK parametrization (see the Appendix). Examples of fits used in the interpolations are given in Figs. 8 and 9. So, for each (m_f, m_q) we first convert the results for $f_\parallel$ and $f_\perp$ of Tables III and IV to f_0 and f_+, interpolate using the BZ ansatz and finally convert back to $f_\parallel$ and $f_\perp$ at fixed values of E_π. These are then extrapolated to the chiral limit using the SChPT formulas described above. One advantage of carrying out interpolations for f_0 and f_+ rather than directly in $f_\parallel$ and $f_\perp$ is that the kinematic constraint $f_0(0) = f_+(0)$ is easily incorporated into the ansaetze and one can use the f_0 data to constrain the normalization of f_+ as well.

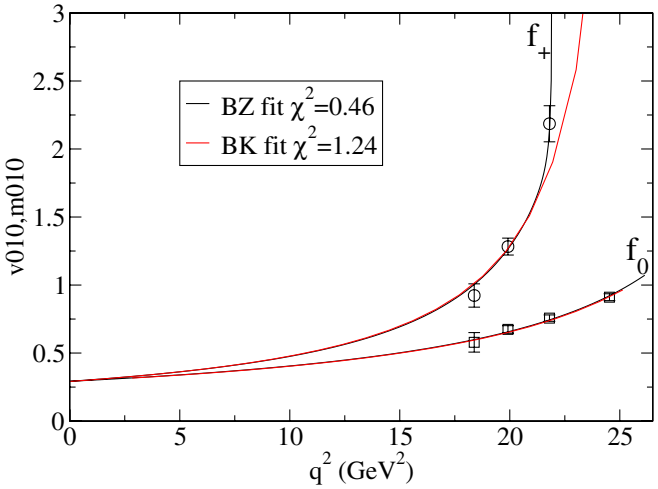

FIG. 8 (color online). Comparison between a 3 parameter BK fit and a 4 parameter BZ fit to $u_0 am_q = u_0 am_f = 0.01$ data.

In Figs. 10 and 11 we show chiral extrapolations for $f_\parallel$ and $f_\perp$, respectively, for several values of E_π. We compare results from simple linear extrapolations of full QCD data and from using the SChPT formulas simultaneously for both full QCD and partially quenched QCD data. One sees that the difference between the two ways of performing the chiral extrapolations is small. For $f_\parallel$ the central values at the chiral limit differ only by 0.1%–2.4%. For $f_\perp$ the differences are again $<$2.4% for $E_\pi > 0.7$ GeV. For $E_\pi \leq 0.7$ GeV (not shown in Fig. 9) linear and SChPT extrapolations of $f_\perp$ can differ by 4%–6%. On the other hand, this is the kinematic region where statistical (and interpolation) errors are large for some combinations of m_f and m_q (see third column in Table IV) and it is not possible to disentangle statistical and chiral extrapolation errors. $f_\perp$ at small E_π translates into f_+ at large q^2. One can speculate that the large statistical errors we are finding in this kine-

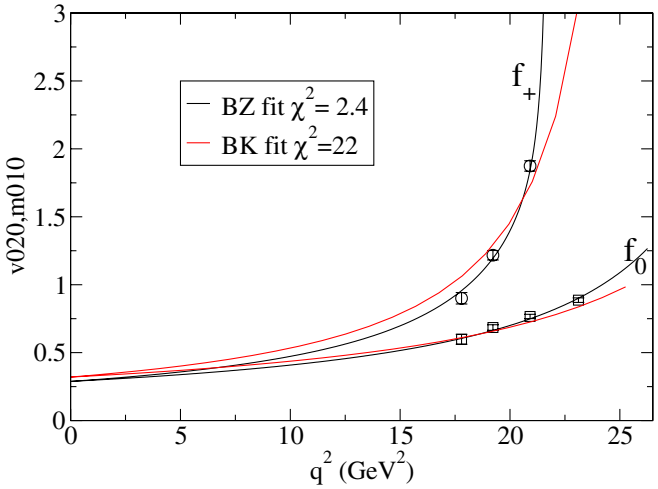

FIG. 9 (color online). Same as Fig. 8 for $u_0 am_q = 0.02$, $u_0 am_f = 0.01$.

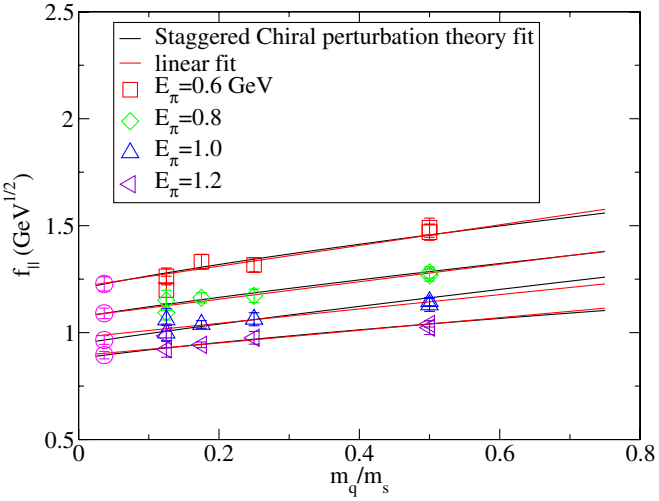

FIG. 10 (color online). Chiral extrapolation of $f_\parallel$. The circles to the left show the extrapolated values at the physical limit.

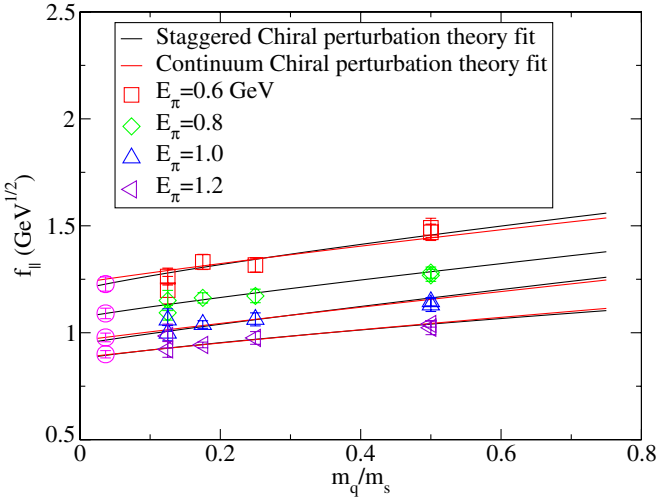

FIG. 12 (color online). Chiral extrapolations with (staggered ChPT) and without (continuum ChPT) $\mathcal{O}(a^2)$ corrections.

matic region may be due to the proximity of the M_{B^*} pole. This, however, for reasons we do not understand, was not evident in the partially quenched data of Ref. [17].

For the SChPT extrapolations, as mentioned above, we have let $g_{B\pi}$ float and be one of the fit parameters. We find that the "effective" $g^2_{B\pi}$ ranges between 0.0 and 0.2 and decreases with E_π, although within large errors. In Fig. 12 we show a comparison of fits with and without the $\mathcal{O}(a^2)$ corrections in the ChPT theory formulas, i.e. a comparison between continuum and staggered full QCD ChPT. Again the differences are very small. In summary, for most of our data points, different ways of carrying out the chiral extrapolation, including using no input from ChPT at all, lead to a spread in extrapolated results of only 2.5% or less. This indicates that contributions we have neglected in the ChPT formulas, such as $1/M$ corrections, higher order (in pion momentum) terms, finite volume effects etc., are not important. We take as central values for the form factors $f_\parallel$ and $f_\perp$ in the chiral limit, the results coming from the SChPT extrapolation using both full QCD and partially quenched data. The combined statistical and chiral extrapolation errors are discussed in the next section.

In Fig. 13 we compare results from one of the MILC fine lattice ensembles with the coarse lattice data discussed so far. For this comparison both the coarse and fine data points include only the $\langle J^{(0)}_\mu \rangle$ contributions through $\mathcal{O}(\alpha_s)$, i.e. the first terms in Eqs. (12) or (13), respectively. Since we have shown that the higher order currents have minimal effect, we believe meaningful scaling tests can be carried out with just $\langle J^{(0)}_\mu \rangle$. For $f_\perp$, which is the main contributor to the phenomenologically relevant form factor $f_+(q^2)$, one sees that the fine lattice point falls nicely on the fixed E_π curve

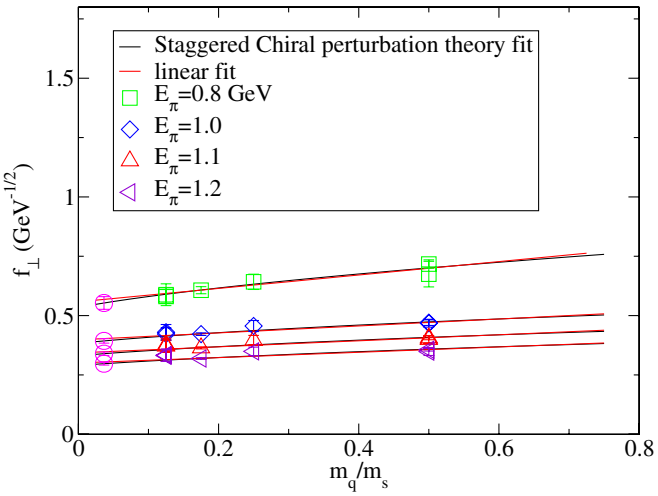

FIG. 11 (color online). Same as Fig. 8 for $f_\perp$.

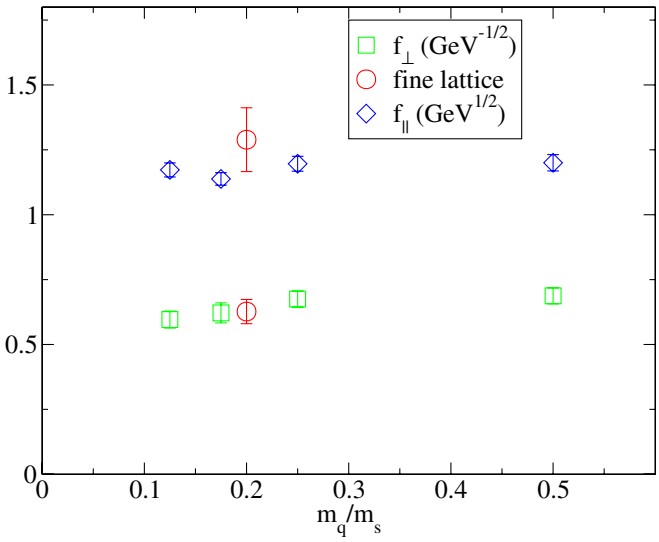

FIG. 13 (color online). Comparison of coarse lattice data with some results from one of the fine MILC ensembles. Shown are results for $f_\perp$ and $f_\parallel$ at $E_\pi = 0.79$ GeV.

determined by coarse lattice data. Our statistical error is large currently for the $f_\parallel$ point from the fine lattice. Within these large errors there is consistency between the coarse and fine lattices for $f_\parallel$ as well. We conclude from this exercise that there are no indications of large discretization effects in the form factor calculations on MILC coarse lattices. Such errors are smaller than current statistical errors. Eventually it would be desirable to carry out a more thorough scaling test, once more data on fine lattices at several light sea quark masses become available.

VI. RESULTS FOR FORM FACTORS $f_+(q^2)$ AND $f_0(q^2)$ IN THE CHIRAL LIMIT

We convert the chirally extrapolated $f_\parallel(E_\pi)$ and $f_\perp(E_\pi)$ to the form factors $f_+(q^2)$ and $f_0(q^2)$ in the physical limit. These are shown in Fig. 14 and tabulated in Table V. For comparison we also plot in Fig. 14 the data presented in Ref. [17]. One sees that changes are minimal in spite of all the improvements included in our new results. This indicates that the approximations that were made previously and that we are systematically improving upon, such as partial quenching, linear chiral extrapolations, working with currents at lowest order in $1/M$, did not drastically affect the theory. The solid curves in Fig. 14 are fits to our new results using the BZ [50] parametrization of f_+ and f_0. We have also tried fits to other parametrizations, described in the Appendix, including the BK [49], Richard Hill (RH) [20] and a series expansion (SE) [19,21,51,52] parametrization. The RH parametrization fit is essentially indistinguishable from the BZ fit. The BK fit is also a good fit to our data although not quite as good as the first two.

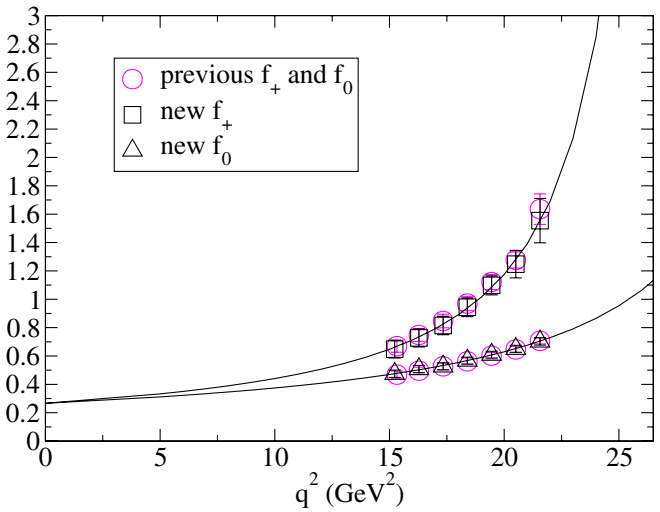

FIG. 14 (color online). Form factors $f_+(q^2)$ and $f_0(q^2)$ in the chiral limit. The black squares and triangles are the new and final results for f_+ and f_0, respectively. For comparison, the data from Ref. [17] are also shown as circles. The full black curves follow a BZ parametrization fit (see text) to the new data. Errors are combined statistical and chiral extrapolation errors.

TABLE V. Form factors $f_+(q^2)$ and $f_0(q^2)$ in the chiral limit. Errors shown are combined statistical and chiral extrapolation errors.

q^2 [GeV^2]	$f_+(q^2)$	$f_0(q^2)$
15.23	0.649(63)	0.475(26)
16.28	0.727(64)	0.508(25)
17.34	0.815(65)	0.527(25)
18.39	0.944(66)	0.568(24)
19.45	1.098(67)	0.610(24)
20.51	1.248(97)	0.651(25)
21.56	1.554(156)	0.703(26)

This should not be surprising, since the BK fit has only three parameters to tune whereas the BZ and RH fits are both 4 parameter fits. Any further parameters, however, are very poorly determined and do not help in the fit. Another class of fit ansatz, the SE fits, are discussed in the Appendix. The main reason we are interested in obtaining a good analytic parametrization of the form factors is to facilitate partial integration of differential decay rates, as discussed below. These parametrizations can also be used to try and extrapolate to lower q^2 where lattice data are currently not available.

The statistical plus chiral extrapolation errors for $f_+(q^2)$ lie between 7% and 10% depending on q^2. They are smaller for the form factor $f_0(q^2)$. For $q^2 \geq 16$ GeV^2, the range we will be focusing on, the average error for $f_+(q^2)$ comes out to be $\sim$8%. In Table VI we list this average statistical plus chiral extrapolation error together with estimates of systematic errors from other sources. These other systematic errors are dominated by the $\sim$9% uncertainty in higher order matching of the heavy-light currents.

The differential partial decay rate for $B \to \pi l \nu$, ignoring the charged lepton mass, is given by

$$\frac{d\Gamma}{dq^2} = \frac{G_F^2}{24\pi^3} p_\pi^3 |V_{ub}|^2 |f_+(q^2)|^2 \qquad (21)$$

where G_F is the Fermi constant and p_π the magnitude of the pion three momentum in the B rest frame. Knowing $f_+(q^2)$ then allows us to evaluate $(1/|V_{ub}|^2)(d\Gamma/dq^2)$ and also integrate this quantity over different q^2 bins. We take our best fit, the BZ fit shown in Fig. 14, and integrate to

TABLE VI. Estimate of percentage errors in $f_+(q^2)$ for $q^2 >$ 16 GeV^2.

Source of error	Size of error (%)
Statistics + chiral extrapolations	8
Two-loop matching	9
Discretization	3
Relativistic	1
Total	12

TABLE VII. Partially integrated differential decay rates and $f_+(0)$ using several parametrizations. The first error reflects statistical and chiral extrapolation uncertainties. The second error is due to remaining systematic errors.

Fit	$f_+(q^2=0)$	$\int \frac{d\Gamma}{dq^2}/\lvert V_{ub}\rvert^2$ [ps^{-1}]	
		$0 \le q^2 \le q^2_{\rm max}$	16 GeV$^2 \le q^2 \le q^2_{\rm max}$
BZ	0.27(2)(4)	6.00(96)(1.68)	1.46(23)(27)
BK	0.26(2)(4)	6.03(96)(1.69)	1.31(21)(25)
RH	0.27(2)(4)	5.99(96)(1.68)	1.45(23)(27)

obtain

$$\frac{1}{|V_{ub}|^2}\int_{16\ \mathrm{GeV}^2}^{q^2_{\rm max}} \frac{d\Gamma}{dq^2}\,dq^2 = 1.46(23)(27)\ \mathrm{ps}^{-1}. \qquad (22)$$

The first error is the combined statistical plus chiral extrapolation error and the second the sum of all other systematic errors added in quadrature. Equation (22) is the main result of this article. It serves as the basis for determinations of the CKM matrix element $|V_{ub}|$. Similar integrals using other parametrizations and over other q^2 ranges are summarized in Table VII together with $f_+(0)$ from the different fits. The second error for $f_+(0)$ and for the integrated rate over the entire q^2 range includes an additional 10% systematic uncertainty in $f_+(q^2)$ which is not part of Table VI and which comes from the extrapolation into the low q^2 region.

VII. ESTIMATING $|V_{ub}|$

In this section we combine the lattice results of the previous section with experimental input for $B \to \pi l \nu$ branching fractions and extract an estimate for $|V_{ub}|$. In order to do so, we use results from the Heavy Flavor Averaging Group (HFAG) [53] and rely on its analysis of the current experimental uncertainties. The HFAG gives preliminary averages of *BABAR*, Belle and CLEO results (as of the conferences of Summer 2005) for the integrated branching fraction $\mathcal{B}\{B^0 \to \pi^- l^+ \nu\}$. They quote $[1.35 \pm 0.08 \pm 0.08] \times 10^{-4}$ for $0 \le q^2 \le q^2_{\rm max}$ and $[0.40 \pm 0.04 \pm 0.04] \times 10^{-4}$ for $q^2 \ge 16$ GeV^2. Combining this with Eq. (22) and a B^0 lifetime of 1.536 ps [54] leads to

$$|V_{ub}| = 4.22(30)(51) \times 10^{-3}, \qquad q^2 \ge 16\ \mathrm{GeV}^2 \quad (23)$$

where the first error is experimental (7%) and the second is the total lattice error (12%). The result (23) is consistent, at the one σ level, with the preliminary value $3.78(25)(52) \times 10^{-3}$ obtained by the Fermilab/MILC Collaboration using the same HFAG branching fraction averages [55].

VIII. SUMMARY

We have completed a determination of the B meson semileptonic form factors $f_+(q^2)$ and $f_0(q^2)$ using state-of-the-art lattice QCD methods. Our calculations employ unquenched gauge configurations, created by the MILC Collaboration, that incorporate vacuum polarization effects from two very light flavors plus strange sea quarks. Both the sea and the valence light quarks are simulated using a highly improved staggered quark action. This action allows us to work close enough to the chiral limit, so that chiral extrapolations to physical pions are mild and do not introduce large uncertainties. Our results for $f_+(q^2)$ can be combined with experimental branching fraction data to extract the CKM matrix element $|V_{ub}|$. This quantity is a crucial ingredient in tests of the unitarity triangle and in solidifying our understanding of CP violation in the standard model.

The total lattice error in the $f_+(q^2)$ form factor presented here, and hence also in $|V_{ub}|$, is at the $\sim$12% level. This error is dominated by uncertainty in higher order perturbative matching of heavy-light currents and by statistical errors. One of the goals of the HPQCD Collaboration is to carry out higher order matching for heavy-light, light-light and heavy-heavy currents and four-fermion operators [56]. It has become increasingly obvious that such calculations are necessary for accurate lattice determinations of form factors, decay constants and mixing parameters at the $\sim$5% level. For form factor calculations, more work is also required to reduce statistical errors. One approach that helped significantly in the HPQCD Collaboration's f_B determination [37] is to explore different smearings of sources and sinks in correlators. We plan to investigate this in the future.

Lattice results for $f_+(q^2)$ exist at the moment only for $q^2 \ge 16$ GeV^2 and this forces us to use only part of the available experimental branching fraction data. In order to take advantage of all the experimental data and thereby reduce experimental errors in $|V_{ub}|$, other methods such as sum rules approaches are currently employed [50,57] to cover the low q^2 region. A lattice approach to $f_+(q^2)$ determinations at low q^2, "moving NRQCD," was introduced many years ago and work is in progress to implement this method using our highly improved quark and gauge actions [58,59]. We can look forward to the next major improvement in lattice determinations of $|V_{ub}|$ once two-loop matching, reduction in statistical errors and control over the entire q^2 range have been achieved.

ACKNOWLEDGMENTS

This work was supported by the DOE and NSF (USA) and by PPARC (UK). A. G., J. S., and M. W. thank the KITP U.C. Santa Barbara for support during the workshop "Modern Challenges in Lattice Field Theory" when part of the present research was carried out. Simulations were done at NERSC and on the Fermilab LQCD cluster. We thank the MILC Collaboration for making their unquenched gauge configurations available and the Fermilab Collaboration for use of their light propagators on the fine lattices. We are grateful to Claude Bernard for

sending us his notes on SChPT for heavy-light form factors. We would also like to acknowledge useful conversations with Richard Hill, Masataka Okamoto, and Iain Stewart.

APPENDIX: PARAMETRIZATION OF FORM FACTORS

Most parametrizations start from a dispersive representation of the form factors.

$$f_+(q^2) = \frac{r_1}{(1-\tilde{q}^2)} + \frac{1}{\pi}\int_{t_+}^{\infty} dt \frac{\mathrm{Im}[f_+(t)]}{t - q^2 - i\epsilon} \rightarrow \frac{r_1}{(1-\tilde{q}^2)} + \frac{r_2}{(1-\alpha\tilde{q}^2)}, \tag{A1}$$

$$f_0(q^2) \rightarrow \frac{r_1 + r_2}{(1-\tilde{q}^2/\beta)} \tag{A2}$$

where $\tilde{q}^2 \equiv q^2/M_{B*}^2$ and $t_+ \equiv (M_B + m_\pi)^2$. The kinematic constraint $f_+(0) = f_0(0)$ is automatically satisfied. This is a 4 parameter parametrization of f_+ and f_0, sometimes called the ''4 parameter BK parametrization'' (Becirevic and Kaidalov) [49]. Examples of generalizations and special cases developed in the literature are given below. They differ only in the parametrization of f_+.

3 parameter BK [49]:

$$f_+(q^2) = \frac{f_+(0)}{(1-\tilde{q}^2)(1-\alpha\tilde{q}^2)}, \tag{A3}$$

$$f_0(q^2) = \frac{f_+(0)}{(1-\tilde{q}^2/\beta)}. \tag{A4}$$

4 parameter BZ [50]:

$$f_+(q^2) = \frac{f_+(0)}{(1-\tilde{q}^2)} + \frac{r\tilde{q}^2}{(1-\tilde{q}^2)(1-\alpha\tilde{q}^2)}. \tag{A5}$$

4 parameter RH [20]:

$$f_+(q^2) = \frac{f_+(0)(1-\delta\cdot\tilde{q}^2)}{(1-\tilde{q}^2)(1-\tilde{q}^2/\gamma)}. \tag{A6}$$

Another class of parametrizations, advocated in [19,51,52] and also discussed in [21], is based on a series expansion of $f_+(q^2)$ around some $q^2 = t_0$. For better convergence of the series it is customary to convert to a new variable $z(q^2, t_0)$, where, following [19,21], we take

$$z(q^2, t_0) = \frac{\sqrt{t_+ - q^2} - \sqrt{t_+ - t_0}}{\sqrt{t_+ - q^2} + \sqrt{t_+ - t_0}}. \tag{A7}$$

We refer to the literature for further discussion of the merits of this transformation. The form factor $f_+(q^2)$ can then be expanded as a power series in $z(q^2, t_0)$,

TABLE VIII. Partially integrated differential decay rates using the SE parametrization for different choices of t_0. No error estimates have been made.

t_0/q^2_{max}	$\int \frac{d\Gamma}{dq^2}/\lvert V_{ub}\rvert^2$ [ps^{-1}]	
	$0 \le q^2 \le q^2_{\mathrm{max}}$	16 GeV$^2 \le q^2 \le q^2_{\mathrm{max}}$
0.0	5.78	1.32
0.2	5.78	1.33
0.4	5.79	1.33
0.6	5.80	1.33
0.8	5.79	1.33
1.0	5.79	1.33

$$f_+(q^2) = \frac{1}{P(q^2)\Phi(q^2, t_0)} \sum_{k=0}^{k_{\mathrm{max}}} a_k(t_0)[z(q^2, t_0)]^k. \tag{A8}$$

The ''Blaschke'' factor $P(q^2)$ must take into account any isolated poles below the $B\pi$ threshold at $q^2 = t_+$. We set $P(q^2) = z(q^2, M_{B^*}^2)$ to take care of the B^* pole. For $\Phi(q^2, t_0)$ we take the expression given in Ref. [19] (with simplified $\chi^{(0)}$). We combine the ansatz (A8) for $f_+(q^2)$ with $k_{\mathrm{max}} = 2$ together with (A4) for $f_0(q^2)$ to get another (and our last) 4 parameter ansatz,

Series expansion:

$$f_+(q^2) = \frac{a_0 + a_1 z(q^2, t_0) + a_2 z^2}{z(q^2, M_{B^*}^2)\Phi(q^2, t_0)}. \tag{A9}$$

We have explored the SE parametrization but not because we needed a better analytic expression to cover the range $q^2 \ge 16$ GeV^2 of our lattice results. Rather, we did so to assess how reliable the information is on the shape of the form factors at lower q^2 that we are getting from the BK/BZ/RH type parametrizations. We find that good fits to the simulation data can be obtained with the SE parametrizations as well and that they are insensitive to the value of t_0. Table VIII gives results for integrated differential decay rates. Not surprisingly, agreement is found with Table VII for $q^2 \ge 16$ GeV^2. Results are systematically slightly lower than in Table VII if one includes the entire q^2 range. One can summarize by saying that we do not have evidence for any strong dependence on the choice of ansatz employed to extrapolate lattice data to lower q^2 values. Nevertheless, we believe it is important to look for additional information on the form factors at $q^2 < 16$ GeV^2, either from experiment or from theoretical models, if one wants to discuss the entire q^2 range at the present time. This has already been done in the recent literature [19,21,50]. Alternatively, getting lattice results directly in the low q^2 regime using, for instance, moving NRQCD would also solve this problem.

[1] B. Aubert *et al.* (*BABAR* Collaboration), Phys. Rev. Lett. **89**, 201802 (2002); **94**, 161803 (2005).

[2] K. Abe *et al.* (Belle Collaboration), Phys. Rev. D **66**, 071102 (2002); Report No. BELLE-CONF-0353 (unpublished), hep-ex/0308036; Report No. BELLE-CONF-0569 (unpublished), hep-ex/0507037.

[3] S. B. Athar *et al.* (CLEO Collaboration), Phys. Rev. D **68**, 072003 (2003).

[4] K. Abe *et al.* (Belle Collaboration), contribution to ICHEP 2004, hep-ex/0408145.

[5] K. Abe *et al.* (Belle Collaboration), contribution to EPS 2005 (unpublished), hep-ex/0508018.

[6] B. Aubert *et al.* (*BABAR* Collaboration), hep-ex/0506064.

[7] B. Aubert *et al.* (*BABAR* Collaboration), Phys. Rev. D **72**, 051102 (2005).

[8] B. Aubert *et al.* (*BABAR* Collaboration), hep-ex/0507085.

[9] For a recent review of inclusive *B* semileptonic decays see U. Nierste, hep-ph/0511125.

[10] For a recent review of exclusive *B* semileptonic decays see I. Stewart, in Proceedings of Lepton-Photon 2005 (unpublished).

[11] K. C. Bowler *et al.* (UKQCD Collaboration), Phys. Lett. B **486**, 111 (2000).

[12] A. Abada *et al.* (APE Collaboration), Nucl. Phys. **B619**, 565 (2001).

[13] S. Aoki *et al.* (JLQCD Collaboration), Phys. Rev. D **64**, 114505 (2001).

[14] A. El-Khadra *et al.* (Fermilab Collaboration), Phys. Rev. D **64**, 014502 (2001).

[15] J. Shigemitsu *et al.*, Phys. Rev. D **66**, 074506 (2002).

[16] M. Okamoto *et al.* (Fermilab/MILC Collaboration), Nucl. Phys. B, Proc. Suppl. **140**, 461 (2005).

[17] J. Shigemitsu *et al.* (HPQCD Collaboration), Nucl. Phys. B, Proc. Suppl. **140**, 464 (2005).

[18] C. Bernard *et al.*, Phys. Rev. D **64**, 054506 (2001).

[19] M. Arnesen *et al.*, Phys. Rev. Lett. **95**, 071802 (2005).

[20] R. Hill, Phys. Rev. D **73**, 014012 (2006).

[21] T. Becher and R. Hill, Phys. Lett. B **633**, 61 (2006).

[22] S. Naik, Nucl. Phys. **B316**, 238 (1989); G. P. Lepage, Phys. Rev. D **59**, 074502 (1999); K. Originos *et al.*, *ibid.* **60**, 054503 (1999); C. Bernard *et al.*, *ibid.* **61**, 111502 (2000).

[23] E. Follana *et al.*, Phys. Rev. Lett. **93**, 241601 (2004); K. Wong and R. Woloshyn, Phys. Rev. D **71**, 094508 (2005); S. Dürr *et al.*, Phys. Rev. D **70**, 094502 (2004); C. Bernard *et al.*, Proc. Sci., LAT2005 (2005) 114 [hep-lat/0509176].

[24] For a recent review see S. Dürr, Proc. Sci., LAT2005 (2005) 021 [hep-lat/0509026].

[25] C. T. H. Davies *et al.*, Phys. Rev. Lett. **92**, 022001 (2004).

[26] C. Aubin *et al.*, Phys. Rev. D **70**, 094505 (2004); **70**, 114501 (2004).

[27] C. Aubin *et al.*, Phys. Rev. D **70**, 031504 (2004).

[28] A. Gray *et al.*, Phys. Rev. D **72**, 094507 (2005).

[29] R. Edwards *et al.*, Phys. Rev. Lett. **96**, 052001 (2006).

[30] I. Allison *et al.*, Phys. Rev. Lett. **94**, 172001 (2005).

[31] C. Aubin *et al.*, Phys. Rev. Lett. **95**, 122002 (2005).

[32] C. Aubin *et al.*, Phys. Rev. Lett. **94**, 011601 (2005).

[33] E. Gulez *et al.*, Proc. Sci., LAT2005 (2005) 220.

[34] C. Bernard, Phys. Rev. D **65**, 054031 (2002); C. Aubin and C. Bernard, Phys. Rev. D **68**, 034014 (2003); **68**, 074011 (2003).

[35] W. Lee and S. Sharpe, Phys. Rev. D **60**, 114503 (1999).

[36] C. Aubin and C. Bernard, Phys. Rev. D **73**, 014515 (2006); C. Bernard (private communication).

[37] A. Gray *et al.*, Phys. Rev. Lett. **95**, 212001 (2005).

[38] M. Wingate *et al.*, Phys. Rev. Lett. **92**, 162001 (2004).

[39] E. Gulez *et al.*, Phys. Rev. D **69**, 074501 (2004).

[40] The NRQCD action used in this article is indeed the same as in [28], which, however, included some typos in the c_2 and c_3 terms of δH. Those typos have been corrected here in Eq. (3).

[41] C. Morningstar and J. Shigemitsu, Phys. Rev. D **57**, 6741 (1998); **59**, 094504 (1999).

[42] S. Collins *et al.*, Phys. Rev. D **63**, 034505 (2001).

[43] Q. Mason *et al.* (HPQCD Collaboration), Phys. Rev. Lett. **95**, 052002 (2005).

[44] M. Wingate *et al.*, Phys. Rev. D **67**, 054505 (2003).

[45] G. P. Lepage *et al.* (HPQCD Collaboration), Nucl. Phys. B, Proc. Suppl. **106**, 12 (2002).

[46] M. Booth, Phys. Rev. D **51**, 2338 (1995); S. Sharpe and Y. Zhang, Phys. Rev. D **53**, 5125 (1996).

[47] D. Becirevic *et al.*, Phys. Rev. D **67**, 054010 (2003); **68**, 074003 (2003).

[48] I. Stewart, Nucl. Phys. **B529**, 62 (1998).

[49] D. Becirevic and A. Kaidalov, Phys. Lett. B **478**, 417 (2000).

[50] P. Ball and R. Zwicky, Phys. Lett. B **625**, 225 (2005).

[51] C. Boyd *et al.*, Phys. Rev. Lett. **74**, 4603 (1995).

[52] C. Boyd and M. Savage, Phys. Rev. D **56**, 303 (1997).

[53] Heavy Flavor Averaging Group, http://www.slac.stanford.edu/xorg/hfag/.

[54] S. Eidelman *et al.* (Particle Data Group), Phys. Lett. B **592**, 1 (2004).

[55] M. Okamoto, Proc. Sci., LAT2005 (2005) 013 [hep-lat/0510113].

[56] H. D. TrottierNucl. Phys. B, Proc. Suppl. **129; 130**, 142 (2004).

[57] P. Ball and R. Zwicky, Phys. Rev. D **71**, 014015 (2005).

[58] S. Hashimoto and H. Matsufuru, Phys. Rev. D **54**, 4578 (1996); J. Sloan, Nucl. Phys. B, Proc. Suppl. **63**, 365 (1998).

[59] K. Foley and P. Lepage, Nucl. Phys. B, Proc. Suppl. **119**, 635 (2003); K. Foley *et al.*, Nucl. Phys. B, Proc. Suppl. **140**, 470 (2005); A. Dougall *et al.*, Proc. Sci., LAT2005 (2005) 219.